Computational Studies of Load-Dependent Guest Dynamics and Free Energies of Inclusion for CO_2 in Low-Density *p-tert*-Butylcalix[4]arene at Loadings up to 2:1

John L. Daschbach, Xiuquan Sun, Tsun-Mei Chang, Praveen K. Thallapally, B. Peter McGrail, and Liem X. Dang*

Pacific Northwest National Laboratory, P.O. Box 999, Richland, Washington 99352, and Department of Chemistry, University of Wisconsin−Parkside, 900 Wood Road, Box 2000, Kenosha, Wisconsin 53141

Received: September 22, 2008; Revised Manuscript Received: February 2, 2009

The structure, dynamics, and free energies of absorption of CO_2 by a low-density structure (*P*4/*n*) of calixarene *p-tert*-butylalix[4]arene (TBC4) at loadings up to 2:1 CO_2:TBC4 have been studied by using molecular dynamics simulations with two sources of initial TBC4 structures (TBC4-T and TBC4-U). The CO_2/TBC4 complex structure is very sensitive to the initial lattice spacing of TBC4. From the computed radial distribution functions of CO_2 molecules, a CO_2 dimer is observed for TBC4-T and a cage-interstitial CO_2 structure is suggested for TBC4-U. The dynamics of the CO_2 molecules show little initial TBC4 structural dependency. The free energy of inclusion for a single CO_2 in this TBC4 structure for various loadings is −4.0 kcal/mol at 300 K and −1.8 kcal/mol at 450 K, showing that CO_2 inclusion is favored. The fully loaded 1:1 CO_2:TBC4 system is slightly less favorable at −3.9 and −1.2 kcal/mol at 300 and 450 K, respectively. The first CO_2 added beyond 1:1 loading shows a significant drop in absorption energy to −1.9 and +1.9 kcal/mol at 300 and 450 K. These data are consistent with experimental results showing that low-density structures of TBC4 are able to absorb CO_2 at loadings greater than 1:1 but retention is lower than for 1:1 loaded systems indicating the free energy of inclusion for addition of the CO_2 above 1:1 is less favorable.

I. Introduction

Supramolecular frameworks with spatial structures lying at the boundary between molecular and nanoscale offer a wide range of possibilities for tailored chemical interactions with other molecules.[1,2] One important area of research and potential application is for the physisorption of gas molecules for separation, sequestration, and storage. As such, they may be important in technological areas such as environmental remediation, synthesis, and clean energy production. In most applications, the ability to reversibly absorb guest molecules is critical since the supramolecular structures are costly to produce, and the ability to reuse them is an important attribute. The infinite possibilities for design of suitable shape, size, and chemical composition host molecules are in many situations a clear advantage of supramolecular structures in comparison with all carbon systems such as carbon nanotubes.[3−6]

A prototypical example with potential real technological application is the inclusion of small guest molecules by calixarene *p-tert*-butylalix[4]arene (TBC4).[7−10] TBC4 is a rigid polyphenolic molecule with a cage-like structure built around four linked phenyl rings. The hemispherical cage in TBC4 is able to absorb a number of small molecules, including CO_2. When crystallized, pure TBC4 molecules form bilayers with the open end of the cage opposed and offset. The crystallized bilayer structure of TBC4 is stable over a wide range of temperatures and pressures. Polymorphs of TBC4 have been crystallized from solution with the inclusion of guest solvent molecules. Recently it has been discovered that high-density TBC4 can absorb CO_2 under suitable conditions of temperature and pressure and change into a low-density form.[5] Furthermore, it has been found that this low-density form becomes metastable when the guest molecules desorb at high temperatures, and may then return to the high-density form. This process of changing between low- and high-density forms can be cycled a number of times. The absorption ability of the TBC4 molecular structures may change with different polymorphs, both through absorption free energies and diffusion transport rates. The energy barrier of the transformation between two polymorphs of the TBC4 crystal is relatively low, which allows for different guest inclusion environments and therefore the possibility of various absorption applications. Recently, an X-ray and NMR study of TBC4 with a CO_2 to TBC4 loading of 1.8:1 was reported by Udachin et al.[10] A transformation of the TBC4 structure from low-density $P2_1/n$ to another low-density *P*4/*n* form driven by the CO_2:TBC4 loading ratio was observed. At higher loading ratio, CO_2 molecules were evenly distributed in cages and interstitial positions. Increasing the temperature can accelerate the rate of CO_2 loading. Also, higher loading of CO_2 can be achieved by increasing the pressure to a higher degree than the conditions used by Udachin et al.[10] There is some uncertainty as to whether the transformation of TBC4 crystal is driven by high loading or by high pressure. It is important to fully understand the microscopic structure and interaction of this system for future functional improvements of host molecules.

Molecular dynamics simulation is a powerful tool to obtain information at the molecular level for chemical systems under conditions where only physical interactions are important, and it has been used to study various guest−host problems. Alavi et al. calculated structural and phase properties for a series of small guest molecules (xenon, sulfur dioxide, nitrogen, methane, carbon dioxide, and hydrogen) captured by TBC4 with molecular dynamics simulations.[11] The absence of guest−guest interactions in neighboring cages is observed for guest/host ratios less than 1:1. They found no correlation between overall rearrangements in the solid state structure and guest inclusion.

* Address correspondence to this author at Pacific Northwest National Laboratory.

10.1021/jp808490g CCC: $40.75
Published on Web 03/12/2009

The energetic interactions between CO_2/H_2 and TBC4 have been studied by using the potential mean force (PMF) for the guest to host interaction in the work of Daschbach et al.[12] These simulations found attractive interactions between CO_2 and TBC4, while repulsive interactions were found between H_2 and TBC4. In addition, the free energy of inclusion for single guest molecules was calculated by using thermodynamic integration for CH_4 and CO_2 in TBC4 and found to be favorable for both guest molecules at temperatures up to 400 K, and decreasing free energy with increasing temperature.[13] Adams and co-workers have used molecular dynamics simulations, augmented with calculations using the potential of mean force technique, to investigate the stability of isolated host−guest complexes and the relationship between the dynamics of these complexes and the dynamics of a solvated host molecule.[14]

In this paper, we explore one low-density TBC4 structure (*P*4/*n*) with a CO_2:TBC4 loadings ratio up to 2:1 at various temperatures using molecular dynamics simulations. The low-density form has a nonoffset layer configuration and the cages are not effectively terminated with a *tert*-butyl group from the opposing layer. The microscopic structure of the system and interactions between CO_2 and TBC4 molecules are investigated by radial distribution function analysis and free energy calculations. Also, the dynamics of the CO_2 guests under different conditions will be investigated with velocity autocorrelation functions. The paper is organized as follows: computational details are given in section II, then simulation results and analysis are discussed in section III, and the conclusion are summarized in section IV.

II. Computational Approach

Calculations were carried out with the sander program from the AMBER version 7 and version 9 molecular dynamics packages.[15,16] We have two sources for the initial coordinates of (*P*4/*n*) TBC4. Both are from X-ray diffraction experiments.[9,10] The two initial (*P*4/*n*) TBC4 structures are the same except for the lattice constants of the unit cell, and will be distinguished by TBC4-T and TBC4-U in our following discussion. A 2 × 2 × 2 replica of the unit cell is used for both of the structures. The resulting dimensions are 25.533 × 25.534 × 25.666 and 25.442 × 25.442 × 25.171 Å^3 for TBC4-T and TBC4-U, respectively.[10] For CO_2, the potential parameters from the Amber 99EP data set were used.[17] A time step of 0.5 fs was used with the SHAKE algorithm to treat the hydrogen vibrations.[18] The short-ranged potential interactions were truncated at 9.0 Å, and long-range electrostatic interactions were treated with the particle mesh Ewald summation technique.[19] Free energies were calculated by thermodynamic integration by using

$$\Delta G = \int_0^\infty \langle \partial V/\partial\lambda \rangle_\lambda \, d\lambda \tag{1}$$

The potential mixing rule was

$$V(\lambda) = (1 - \lambda)^k V_0 + [1 - (1 - \lambda)^k] V_1 \tag{2}$$

where V_0 is the unperturbed Hamiltonian and V_1 is the perturbed Hamiltonian with $k = 4$ to treat the divergence of the integral in eq 1 when atoms are created and destroyed. For all systems, $\partial V/\partial\lambda$ was calculated with 13 different values of λ. Thermodynamic integration runs in the NPT ensemble were 2.5 ns for $\lambda < 0.85$ and 3.5 ns for $\lambda > 0.85$ with the first 100 ps of each calculation used for equilibration. Integration of the free energy used a weighted quadratic polynomial.

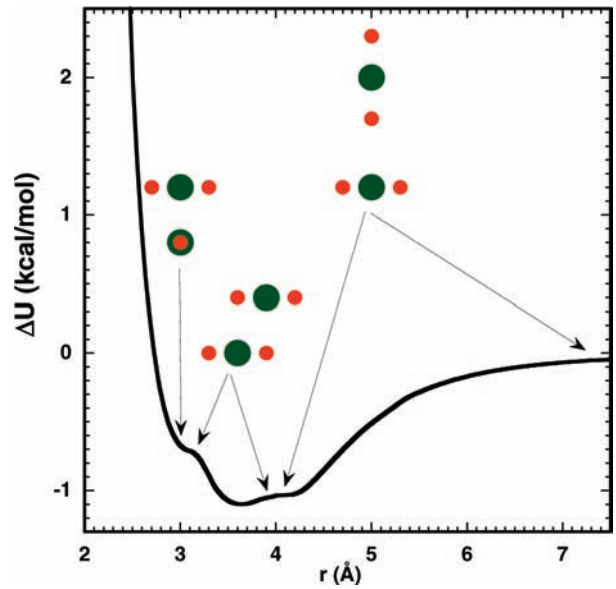

Figure 1. The computed CO_2−CO_2 gas phase dimer potential energy curve as a function of center of mass separation.

The structural properties of the system were investigated by calculating radial distribution functions (RDF). The dynamics of the guest motion in the TBC4 cage was investigated by using the velocity autocorrelation function (VACF), given by

$$C(t) = \langle V(t) \bullet V(0) \rangle \tag{3}$$

where $V(t)$ and $V(0)$ are the center-of-mass and angular velocities (translational or rotational) of CO_2 molecules at time t and time 0. The angular brackets denote an ensemble average. The corresponding spectral density is defined as:

$$f(\omega) = \int_0^\infty e^{-i\omega t} C(t) \, dt \tag{4}$$

Each system was equilibrated for 100 ps with use of NTP conditions and then 100 ps of dynamics were recorded under NVE conditions with a time step of 0.5 fs with sampling at 5 fs intervals.

III. Results and Discussion

We begin this section by examining the potential energy surface for the CO_2 dimer due to its importance in CO_2 loading. The computed CO_2−CO_2 dimer potential energy curve is shown in Figure 1. The curve shows the lowest energy configuration for each distance r. The minimum is at 3.65 Å with an energy of −1.10 kcal/mol, and the configuration is the slipped parallel geometry as found in crystalline CO_2. At a CO_2 distance of 3 Å, the dimer is found to be attractive with −0.67 kcal/mol stabilization in the crossed geometry as shown in Figure 1. At separations >4.2 Å the configuration changes to a T-shaped configuration. A high-level electronic structure calculation of the dimer potential for different geometries shows a set of potential curves crossing in the 3 to 4.2 Å region.[20] By using a simple CO_2 potential this calculation closely follows the lowest energy path found in the high-level calculation for the dimer structure with respect to distance. As a check, calculations of pure liquid CO_2 using the potential employed in this work yield

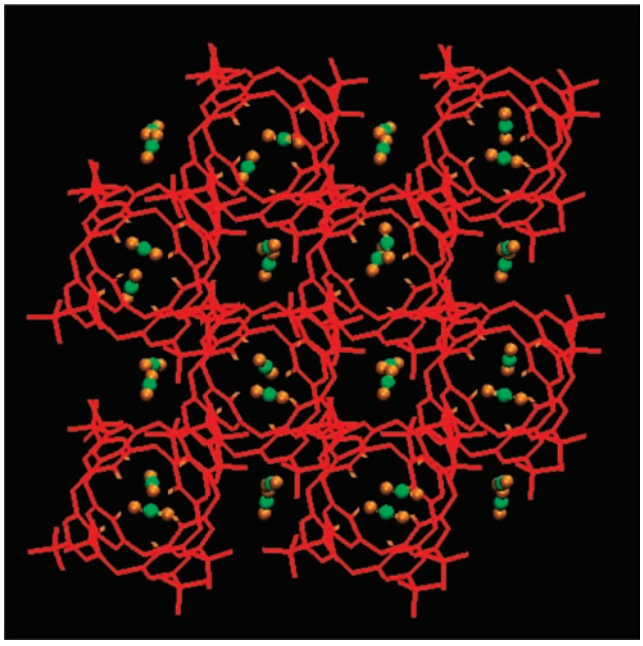

Figure 2. A snapshot taken from MD simulations for the CO_2/TBC4 system.

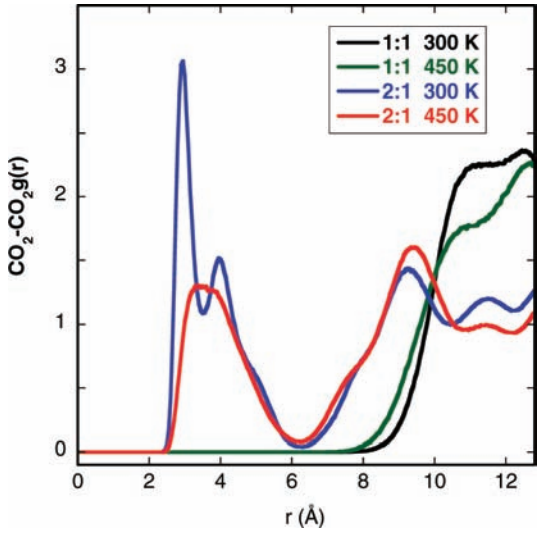

Figure 3. Radial distribution function for the CO_2-CO_2 center of mass for CO_2 loadings of 1:1 and 2:1 in TBC4-T at 300 and 450 K.

the first carbon−carbon peak close to 4 Å at densities between 0.8 and 1.4 g/cm^3, in agreement with other experimental and computational results.[21−23]

A. Structure. In Figure 2, we present a snapshot for the 2:1 CO_2:TBC4 loading in TBC4-T after equilibration. Figure 3 shows the calculated radial distribution functions for the center of mass between two CO_2 molecules for loading ratios of 1:1 and 2:1 at 300 and 450 K in TBC4-T. The data were obtained by sampling at 1 ps intervals over the total dynamics trajectory of 3.5 ns after 2 ns of equilibration. The 1:1 loading ratio peak of TBC4-T shows a single broad peak from the caged CO_2 separation. At the higher temperature, the peak is only slightly broadened from the 300 K peak and the shoulder around 11 Å is reduced. No evidence is found for CO_2 outside the cage, but the width shows that CO_2 molecules are relatively free inside the cages.

The RDF for 2:1 loading ratios of TBC4-T is quite different. A striking result is that for ratios above 1:1, CO_2 pairs are found

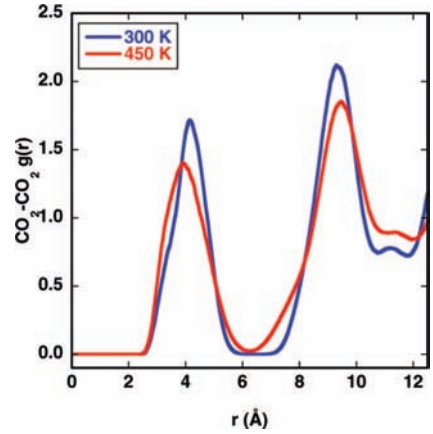

Figure 4. Radial distribution function for the CO_2-CO_2 center of mass for CO_2 loadings of 2:1 in TBC4-U at 300 and 450 K.

in the cages, occupying the same region of the cage as a single monomer would, which is evident from the first RDF peak, and also the snapshot shown in Figure 3. Also, the dimer center of mass separation is found to be near 3 Å, which is 0.65 Å closer than that found in the gas-phase dimers discussed in Figure 1. At 300 K, the RDF shows a prominent sharp peak around 3 Å, a second peak around 4 Å, and a much broader band from 7 to 12 Å. At 450 K, the finer structure of the first two peaks is lost, but the overall coarse structure remains largely the same. Merging of the first two peaks indicates that at 450 K the CO_2 pairs explore more phase space. The center of mass separation is significantly smaller than that found in pure liquid or solid CO_2 under normal/nonextreme conditions. Neutron diffraction studies and molecular dynamics studies in fluid CO_2 between 240 and 473 K at densities between 1.0 and 1.3 g/cm^3 show the first g_{cc} peak between 4.05 and 4.15 Å.[21,23] Simulations of solid CO_2 at 85 K and 1 atm show the first peak in the g_{cc} at 4 Å, in agreement with the X-ray crystal structure at 150 K with a C−C distance of 3.8 Å.[24] The CO_2 dimers are stabilized by the cages so that they are closer to each other than the distance of energy global minimum in Figure 1 and the distance found in condensed phase CO_2.

The RDF shown in Figure 4 for a loading ratio of 2:1 for TBC4-U at 300 K indicates a strong peak at 4.1 Å, and a weak shoulder peak around 3.3 Å. It has a much larger separation than the CO_2 dimers in TBC4-T, indicating a significantly different CO_2−TBC4 complex structure. The strong peak at 4.1 Å is assigned to the distance between CO_2 molecules in the cage and interstitial positions. This distance is close to the C−C distance measured in experiment and the global minimum in our CO_2 dimer energy calculation. The CO_2 molecules at the interstitial positions are stabilized by the *tert*-butyl functional groups of the TBC4 molecules consistent with experimental and simulation results at much lower temperatures.[10,11] At 450 K, the first peak is shifted to a shorter distance of ~4 Å. As we mentioned above, the two initial structures for TBC4 are similar to each other, with dimensions of 25.533 × 25.534 × 25.666 and 25.442 × 25.442 × 25.171 Å for TBC4-T and TBC4-U simulation boxes, respectively. The TBC4-T has a more expanded structure than TBC4-U, especially for the *z*-axis, in which there is a 0.5 Å difference. We can also see that the CO_2/TBC4 complex structure is very sensitive to the initial states in our molecular dynamics simulations. With higher temperature, the structural differences smear out. The volumes of simulation boxes are expanded to 18 019 and 18 007 Å^3 for TBC4-T and TBC4-U, respectively, at 450 K. Compared to the volume difference between 17 332 and 17 154 Å^3 at 300 K, the volumes

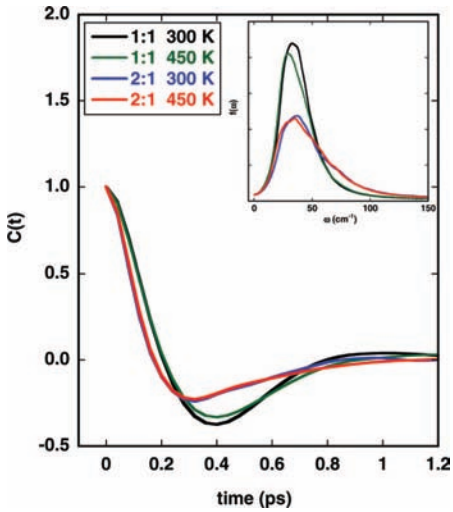

Figure 5. Translational velocity autocorrelations for CO_2 center of mass for 1:1 and 2:1 CO_2 in TBC4 at 300 and 450 K. The inset is the corresponding translational spectra.

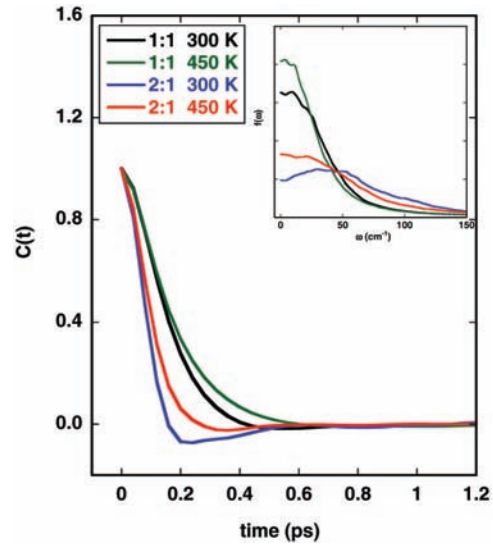

Figure 6. Rotational velocity autocorrelations for CO_2 center of mass for 1:1 and 2:1 CO_2 in TBC4 at 300 and 450 K. The inset is the corresponding rotational spectra.

are almost the same at 450 K, and the corresponding RDFs are very similar to each other. The two different initial structures start to converge to the same state at high temperature. Apparently, the energy barrier for the phase transformation is too high to be overcome at the lower temperature, but can be at the higher temperature.

B. Dynamics. Figure 5 shows translational velocity autocorrelation functions for CO_2 molecules with a loading ratio of 1:1 and 2:1 in TBC4-T at 300 and 450 K. The dampings are less for systems with 16 CO_2 molecules (loading of 1:1) during the initial simulation period. This is evidence of two-body coupling; the only force is due to the interaction between the CO_2 molecule and the wall of the cage of TBC4 for a loading of 1:1. This is consistent with the results from other studies.[11] For a loading of 2:1, due to the existence of CO_2 pairs, the translation of CO_2 is perturbed by another CO_2 molecule in the same cage. Shown as an inset in Figure 5 is the corresponding spectral density calculated from the VACF. One dominant frequency around 40 cm^{-1} is assigned to the rattling mode of the CO_2 molecules. The peak frequencies are almost the same for 1:1 and 2:1 loadings at the same temperature. However, the peak shifts to lower frequency with increasing temperature implying that the rattling of CO_2 molecules in the TBC4 cage results from the coupling between the CO_2 molecule and the wall of the cage of TBC4. This phenomenon is observed for other systems by using both experiment and simulation.[25,26]

Figure 6 shows the rotational VACF for the CO_2 molecules in TBC4-T. Unlike the translation, the relaxing times for rotation at 1:1 and 2:1 loadings are quite different, the CO_2 molecules rotate much faster at 2:1 than at 1:1. The spectral densities calculated from rotation VACF of CO_2 molecules are also presented in Figure 6. Besides the observed perturbation by CO_2 clusters, the spectrum also shows temperature dependency for 2:1 loading. At low temperature (300 K), one broad peak is located around 40−50 cm^{-1}. At high temperature (450 K), only a small shoulder is present around 20 cm^{-1}. The effects to the rotation of the CO_2 molecules at 2:1 loading arise from two factors: (1) the interaction between CO_2 and TBC4 molecules and (2) the interaction between CO_2 neighbor molecules. From the dimer energy calculation, the relative orientation of the neighboring CO_2 molecules is very sensitive to the distance between each other. At low temperature, this orientational preference dominates the rotation of the CO_2 molecules. At high temperature, the CO_2 molecules rotate more freely, and the spectral density becomes similar to the 1:1 case for which the interaction between CO_2 molecules is negligible due to the large separation between them.

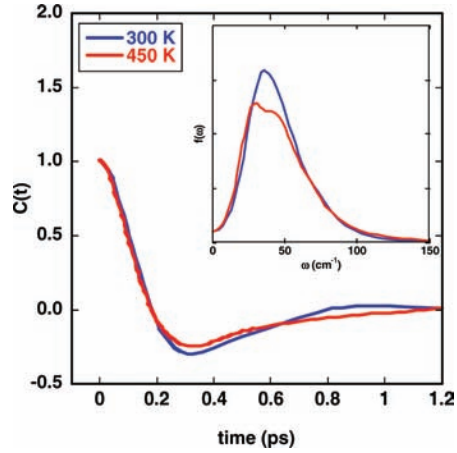

Figure 7. Translational velocity autocorrelations for CO_2 center of mass for 2:1 CO_2 in TBC4-U at 300 and 450 K. The inset is the corresponding translational spectra.

Figure 7 shows the translational VACF of CO_2 molecules for 2:1 loading in TBC4-U at 300 and 450 K. The VACF are very similar to each other at both temperatures. Compared to the VACF of CO_2 in TBC4-T, little difference is observed. For the spectral density, the dominant frequency is around 40 cm^{-1}. This is the same as that for the CO_2/TBC4-T complex. Additionally, the peak also shifts to lower frequency with increasing temperature. Figure 8 shows the rotational VACF of CO_2 molecules for a 2:1 loading in TBC4-U at 300 and 450 K. The corresponding spectra are shown in the inset. The same temperature dependence for the rotation of CO_2 molecules as found in the 2:1 loading in TBC4-T is observed. The peak frequencies in the spectra are 45 and 20 cm^{-1} for 300 and 450 K, respectively. These are very close to the frequencies calculated for the CO_2/TBC4-T complex.

Upon comparing the dynamical properties of the CO_2 molecules in CO_2/TBC4-T and CO_2/TBC4-U complexes at different temperatures, we find little structural dependence. For the CO_2/TBC4-U complex, the environments are quite different

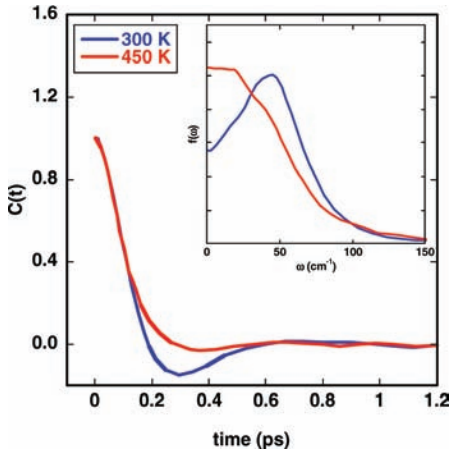

Figure 8. Rotational velocity autocorrelations for CO_2 center of mass for 2:1 CO_2 in TBC4-U at 300 and 450 K. The inset is the corresponding rotational spectra.

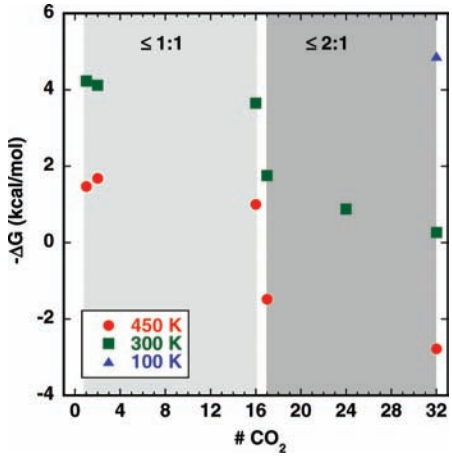

Figure 9. Gibbs free energy of inclusion for one CO_2 molecule in TBC4 for various CO_2 loadings (16 is 1:1 and 32 is 2:1 with respect to TBC4) at 300 and 450 K.

for the CO_2 molecules in the cage and interstitial positions; however, only one dominant frequency is observed in both the translational and rotational spectra. This suggests a fast exchange of CO_2 molecules between the two different sites, and is confirmed by our visible inspection of the molecular dynamics trajectories. A similar conclusion was reported by NMR spectroscopy.[10]

C. Free Energy Calculations. Figure 9 shows the Gibbs free energy of inclusion with various loadings of CO_2 in TBC4-T at 300 and 450 K. The periodic system has 16 TBC4 molecules so that a loading of 16 CO_2 corresponds to the fully loaded 1:1 system and 32 CO_2 corresponds to the fully loaded 2:1 system (a snapshot is shown in Figure 2). For each system, a single CO_2 molecule was perturbed. The initial structure was from a 2 ns dynamics run with unperturbed CO_2 for the 1:1 (16 CO_2) system at 300 K with a single CO_2 molecule initially placed in each TBC4 cage. For loadings above 1:1 the equilibrated 1:1 structure was used as a starting point. Additional CO_2 molecules were placed in the interstitial sites as suggested in ref 10. A locally stable location for the interstitial site was found by testing a series of initial configurations for a single interstitial CO_2 followed by minimization. This location was replicated for higher loadings, with minimization for each system. Thermodynamic integration (TI) runs were performed for 2.5 or 3.5 ns at 13 values of the perturbation parameter, λ, with the longer runs used at either end of the perturbation series where the $\partial V/\partial\lambda$ distributions were slower to converge. The first 100 ps of data were used for equilibration. For loadings up through 1:1 (1 to 16 CO_2 molecules) the CO_2 molecules reside one to a cage and inspection of trajectory shows no evidence of cage hopping on the time scale of the simulation at these temperatures. For higher loadings (17 to 32 CO_2 molecules) we observed in dynamics runs and in the final configurations of the TI runs that the CO_2 locations are dynamic at these temperatures. As discussed previously, occupancy of a cage by 2 CO_2 molecules appears favored over one being in the interstitial site, resulting in additional CO_2 molecules being indistinguishable from initially caged CO_2 molecules once a cage is occupied by two CO_2 molecules. Because the calculation perturbs only a single CO_2, this liability makes sampling of the loadings greater than 1:1 less complete. It might be expected that the overall change in potential energy with perturbation would be different when the perturbed molecule was resident as a single CO_2 in a TBC4 cage, in an interstitial position, or when it is clustered with a second CO_2. Inspection of the potential energy fluctutations indicates this is likely occurring, as the TI runs with only slightly perturbed CO_2 sometimes show overlapping but discernible bands of $\partial V/\partial\lambda$ sampling. The transitions appear to occur over windows of less than 10 ps but the lifetimes of the apparently different states can be long, 100 to 1000 ps, on the same order as the total simulation time. The uncertainty in the free energy calculations is estimated to be on the order of ± 1 kcal/mol.

The data in Figure 9 show that the inclusion of CO_2 is favored at low loadings and lower temperatures. The temperature dependence, with absorption being less favorable at high temperature, shows the enthalpy contribution to inclusion is more important than the entropic component. This is expected, as the cage in which the CO_2 solvates is already present, even without a CO_2 being close at hand, and because the cage is relatively stiff, resulting in little to no cage rearrangement upon inclusion of the guest. The calculation starts with the cage structure of the fully loaded 1:1 system, and so corresponds only to absorption into the metastable low-density empty TBCA form similar to previous work.[5]

The small decrease in free energy going from a loading of 1:16 to 1:1 (16 CO_2) is slightly puzzling. Up to the 1:1 case, the CO_2 molecules appear to remain in a single cage, and the interaction between CO_2 molecules should be very small. They are being absorbed into the low-density 2:1 TBC4 structure, so rearrangement of the TBC4 structure should be negligible. The differences between the 1:16 and 2:16 loadings and the 1:1 loading are within the estimated uncertainty in the calculation, and so inferring anything from the observed decrease is not supported.

At 300 K, the free energy of inclusion is -4 kcal/mol compared with our earlier calculation for the absorption of a single CO_2 in the high-density form of TBC4 of -5.4 kcal/mol.[13] Even with the relatively large uncertainty, it appears absorption in the low-density form is slightly favored. The difference is likely due to the interaction with the *tert*-butyl group, which caps the cage in a high-density form, leading to a more spherical cage.

There is a noticeable decrease in the absorption free energy upon introducing the first CO_2 molecule beyond the 1:1 loading, starting with the 17th CO_2 molecule. At 300 K the absorption remains favorable, but at 450 K it becomes unfavorable. This is expected, as storing crystals loaded above 1:1 at room temperature results in a loss of the interstitial molecules within 5 days, while loss of the caged CO_2 molecules under the same conditions was not complete (8% caged CO_2 remaining) after

60 days.[10] With respect to energetics, the trends in the calculations conform to the experimental observations. The inclusion energy for the 2:1 system at 300 K is slightly favorable by −0.4 kcal/mol but unfavorable by 2.8 kcal/mol at 450 K (see the discussion below). This result is intriguing because it suggests the possibility for the design of supramolecular structures with favorable mass loadings and controlled absorption/desorption under reasonable conditions.

The decrease in free energy is more pronounced with loading above 1:1. NMR results for systems loaded above 1:1 show only a single peak for CO_2, although the environment for CO_2 in cages and in interstitial sites is sufficiently different that two NMR peaks are expected.[10] It is postulated that this is a result of the rapid exchange of CO_2 between the cage and interstitial positions. The dynamics of the CO_2 exchange would then lead to entropic effects, since an interstitial site can exchange with more than one symmetric cage site.

The calculations support the loadings of greater than 1:1 for CO_2 in the low-density form TBC4 at 300 K, consistent with experiments.[5] The loading and temperature trends are not surprising. However, the molecular dynamics calculations have an interesting feature different from the experimental interpretation, which is at least partially consistent with the NMR results: that pairs of CO_2 molecules cluster in cages at higher loadings.

IV. Conclusion

We have carried out molecular dynamics simulations on the CO_2:TBC4 system with two initial TBC4 structures, TBC4-T and TBC4-U. We studied the structure, dynamics, and free energies of absorption of CO_2 by a low-density structure of TBC4 (*P*4/*n*) at loadings up to 2:1 CO_2:TBC4. The CO_2/TBC4 complex structure is very sensitive to the initial state of TBC4. For loadings of 2:1, the CO_2 structure is primarily dimers with a mean center of mass separation of 3 Å located at the same position along the cage axis in TBC4, and as monomers in the 1:1 CO_2:TBC4-T system. For a 2:1 loading ratio, the CO_2 molecules are stable on both cage and interstitial positions with a mean center of mass separation of 4.1 Å in the CO_2/TBC4-U system. A gas-phase calculation for the CO_2 dimer potential energy shows the minimum at −1.10 kcal/mol with a separation of 3.65 Å in the slipped parallel geometry and −0.67 kcal/mol at 3 Å in the crossed geometry. In the 2:1 loaded CO_2:TBC4 system, the CO_2 dimer is sufficiently stabilized by the interaction with the TBC4 to favor a structure 0.43 kcal/mol higher than the vacuum minimum. The dimer structure for CO_2 absorbed in TBC4 has not been reported, but the present study suggests this is energetically possible for low-density TBC4 structures.

Unlike the structure of the CO_2:TBC4 system, the dynamical properties of the CO_2 molecules show little initial TBC4 structural dependence. Translational velocity autocorrelation calculations show a single peak under all conditions studied with very little change in temperature. Rotational velocity autocorrelation calculations show relatively little structure, with significant tailing to low frequencies indicating rotation is hindered in the conical TBC4 cavity in the low-density structure.

The free energy of inclusion for CO_2 in this TBC4-T structure at 300 and 450 K for various loadings shows the inclusion of a single CO_2 in the system is favorable by −4.0 kcal/mol at 300 K and −1.8 kcal/mol at 450 K. The fully loaded 1:1 CO_2:TBC4 system is slightly less favorable by −3.9 and −1.2 kcal/mol for 300 and 450 K, respectively. The first CO_2 added beyond 1:1 loading shows a significant drop in absorption energy to −1.9 and +1.9 kcal/mol at 300 and 450 K. These data are consistent with experimental results showing that low-density structures of TBC4 are able to absorb CO_2 at loadings greater than 1:1, but retention is lower than for 1:1 loaded systems, indicating the energy of inclusion for addition of the CO_2 above 1:1 is less favorable.

Acknowledgment. This work was performed at the Pacific Northwest National Laboratory (PNNL) and was supported by the Division of Chemical Sciences, Office of Basic Energy Sciences, U.S. Department of Energy (DOE). PNNL is operated by Battelle for the DOE. P.B.M. and J.L.D. gratefully acknowledge support received from the National Energy Technology Laboratory of DOE's Office of Fossil Energy.

References and Notes

(1) Atwood, J. L.; Barbour, L. J.; Jerga, A. *Science* **2002**, *296*, 2367.
(2) Enright, G. D.; Udachin, K. A.; Moudrakovski, I. L.; Ripmeester, J. A. *J. Am. Chem. Soc.* **2003**, *125*, 9896.
(3) Dalgarno, S. J.; Thallapally, P. K.; Barbour, L. J.; Atwood, J. L. *Chem. Soc. Rev.* **2007**, *36*, 236.
(4) Soldatov, D. V.; Moudrakovski, I. L.; Ripmeester, J. A. *Angew. Chem., Int. Ed.* **2004**, *43*, 6308.
(5) Thallapally, P. K.; Dobrzanska, L.; Gingrich, T. R.; Wirsig, T. B.; Barbour, L. J.; Atwood, J. L. *Angew. Chem., Int. Ed.* **2006**, *45*, 6506.
(6) Zyryanov, G. V.; Rudkevich, D. M. *J. Am. Chem. Soc.* **2004**, *126*, 4264.
(7) Ripmeester, J. A.; Enright, G. D.; Ratcliffe, C. I.; Udachin, K. A.; Moudrakovski, I. L. *Chem. Commun.* **2006**, 4986.
(8) Thallapally, P. K.; McGrail, B. P.; Atwood, J. L.; Gaeta, C.; Tedesco, C.; Neri, P. *Chem. Mater.* **2007**, *19*, 3355.
(9) Thallapally, P. K.; McGrail, B. P.; Dalgarno, S. J.; Schaef, H. T.; Tian, J.; Atwood, J. L. *Nat. Mater.* **2008**, *7*, 146.
(10) Udachin, K. A.; Moudrakovski, I. L.; Enright, G. D.; Ratcliffe, C. I.; Ripmeester, J. A. *Phys. Chem. Chem. Phys.* **2008**, *10*, 4636.
(11) (a) Alavi, S.; Afagh, N. A.; Ripmeester, J. A.; Thompson, D. L. *Chem.−Eur. J.* **2006**, *12*, 5231. (b) Alavi, S.; Ripmeester, J. A. *Chem. Eur. J.* **2008**, *14*, 1965.
(12) Daschbach, J. L.; Thallapally, P. K.; Atwood, J. L.; McGrail, B. P.; Dang, L. X. *J. Chem. Phys.* **2007**, 127.
(13) Daschbach, J. L.; Thallapally, P. K.; McGrail, B. P.; Dang, L. X. *Chem. Phys. Lett.* **2008**, *453*, 123.
(14) Adams, J. E.; Cox, J. R.; Christiano, A. J.; Deakyne, C. A. *J. Phys. Chem. A* **2008**, *112*, 6829.
(15) Case, D. A.; Pearlman, D. A.; Caldwell, J. W.; Cheatham, T. E., III.; Wang, J.; Ross, W. S.; Simmerling, C. L.; Darden, T. A.; Merz, K. M.; Stanton, R. V.; Cheng, A. L.; Vincent, J. J.; Crowley, M.; Tsui, V.; Gohlke, H.; Radmer, R. J.; Duan, Y.; Pitera, J.; Massova, I.; Seibel, G. L.; Singh, U. C.; Weiner, P. K.; Kollman, P. A. *AMBER 7*; University of California, San Francisco, CA, 2002.
(16) Case, D. A.; Darden, T. A.; Cheatham, T. E., III.; Simmerling, C. L.; Wang, J.; Duke, R. E.; Luo, R.; Merz, K. M.; Pearlman, D. A.; Crowley, M.; Walker, R. C.; Zhang, W.; Wang, B.; Hayik, S.; Roitberg, A.; Seabra, G.; Wong, K. F.; Paesani, F.; Wu, X.; Brozell, S.; Tsui, V.; Gohlke, H.; Yang, L.; Tan, C.; Mongan, J.; Hornak, V.; Cui, G.; Beroza, P.; Mathews, D. H.; Schafmeister, C.; Ross, W. S.; Kollman, P. A. *AMBER 9*; University of California, San Francisco, CA, 2006.
(17) Wang, J. M.; Wolf, R. M.; Caldwell, J. W.; Kollman, P. A.; Case, D. A. *J. Comput. Chem.* **2004**, *25*, 1157.
(18) van Gunsteren, W. F.; Berendsen, H. J. C. *Mol. Phys.* **1977**, *34*, 1311.
(19) Duke, R. E.; Pedersen, L. G. *PMEMD 3*; University of North Carolina−Chapel Hill, 2003.
(20) Bukowski, R.; Sadlej, J.; Jeziorski, B.; Jankowski, P.; Szalewicz, K. *J. Chem. Phys.* **1999**, *110*, 3785.
(21) Cipriani, P.; Nardone, M.; Ricci, F. P.; Ricci, M. A. *Mol. Phys.* **2001**, *99*, 301.
(22) Ishii, R.; Okazaki, S.; Okada, I.; Furusaka, M.; Watanabe, N.; Misawa, M.; Fukunaga, T. *J. Chem. Phys.* **1996**, *105*, 7011.
(23) Zhang, Z. G.; Duan, Z. H. *J. Chem. Phys.* **2005**, 122.
(24) Nishikawa, K.; Takematsu, M. *Chem. Phys. Lett.* **1994**, *226*, 359.
(25) Chazallon, B.; Itoh, H.; Koza, M.; Kuhs, W. F.; Schober, H. *Phys. Chem. Chem. Phys.* **2002**, *4*, 4809.
(26) Tse, J. S.; Klug, D. D.; Zhao, J. Y.; Sturhahn, W.; Alp, E. E.; Baumert, J.; Gutt, C.; Johnson, M. R.; Press, W. *Nat. Mater.* **2005**, *4*, 917.

JP808490G